OPEN

# Input of terrestrial organic matter linked to deglaciation increased mercury transport to the Svalbard fjords

Haryun Kim[1], Sae Yun Kwon[2], Kitack Lee[2], Dhongil Lim[3], Seunghee Han[4], Tae-Wook Kim[5], Young Ji Joo[6], Jaesoo Lim[7], Moo-Hee Kang[8] & Seung-Il Nam[6]*

Deglaciation has accelerated the transport of minerals as well as modern and ancient organic matter from land to fjord sediments in Spitsbergen, Svalbard, in the European Arctic Ocean. Consequently, such sediments may contain significant levels of total mercury (THg) bound to terrestrial organic matter. The present study compared THg contents in surface sediments from three fjord settings in Spitsbergen: Hornsund in the southern Spitsbergen, which has high annual volume of loss glacier and receives sediment from multiple tidewater glaciers, Dicksonfjorden in the central Spitsbergen, which receives sediment from glacifluvial rivers, and Wijdefjorden in the northern Spitsbergen, which receive sediments from a mixture of tidewater glaciers and glacifluvial rivers. Our results showed that the THg ($52 \pm 15 \, \mathrm{ng \, g^{-1}}$) bound to organic matter (OM) was the highest in the Hornsund surface sediments, where the glacier loss ($0.44 \, \mathrm{km^3 \, yr^{-1}}$) and organic carbon accumulation rates ($9.3 \sim 49.4 \, \mathrm{g \, m^{-2} \, yr^{-1}}$) were elevated compared to other fjords. Furthermore, the $\delta^{13}C$ ($-27 \sim -24\permil$) and $\delta^{34}S$ values ($-10 \sim 15\permil$) of OM indicated that most of OM were originated from terrestrial sources. Thus, the temperature-driven glacial melting could release more OM originating from the meltwater or terrestrial materials, which are available for THg binding in the European Arctic fjord ecosystems.

Increasing temporal trends of total mercury (THg) concentration in the sediments of the Arctic continental shelves and lakes have recently been reported[1,2]. These increasing levels have been proposed to be caused by the long-distance transport of anthropogenic mercury (Hg) from industrialized countries to the Arctic, given its long atmospheric lifetime of 0.3 to 2 years[3,4]. In addition, it has been shown that 'Atmospheric Mercury Depletion Events' (AMDE) in the spring can lead to high Hg deposition in the Arctic Ocean. Reactive Hg ($Hg^{2+}$) is rapidly formed through *in situ* oxidation of gaseous Hg° by halogens (i.e., atomic Br and radical BrO), which are generated by solar irradiation through $O_3$ destruction[5–7]. However, previous measurements of atmospheric Hg deposition in the Arctic regions have revealed relatively low deposition rates of $<5 \, \mathrm{\mu g \, m^{-2} \, yr^{-1}}$[8]. Recent studies have suggested that natural processes governing Hg release via riverine transport[9], soil runoff, and/or discharge of water coming from thawing permafrost[10] could be important sources of Hg to the Arctic environments.

Fjords on Svalbard, the main island of the Svalbard archipelago, is among the most studied fjord systems in the world[11]. Previous studies have focused on the effects of local and/or long-range transport, oceanic currents, and long-term sediment deposition rates (i.e., geological and chemical processes that control Hg distribution in surface and core sediments)[4,12–17] on spatial distribution and the extent of accumulation of Hg in the fjord sediment. Recent studies have shown that fjords are effective sequesters of organic carbon among other marine

[1]Fundamental Research Division, National Marine Biodiversity Institute of Korea, 33662, Janghang, South Korea. [2]Division of Environmental Science and Engineering, Pohang University of Science and Technology, 37673, Pohang, South Korea. [3]South Sea Research Institute, Korea Institute of Ocean Science and Technology, 53201, Geoje, South Korea. [4]School of Earth Sciences and Environmental Engineering, Gwangju Institute of Science and Technology (GIST), 61005, Gwangju, South Korea. [5]Division of Environmental Science and Ecological Engineering, Korea University, 02841, Seoul, South Korea. [6]Division of Polar Paleoenvironment, Korea Polar Research Institute, 21990, Incheon, South Korea. [7]Geological Research Division, Korea Institute of Geosciences and Mineral Resources, 34132, Daejeon, South Korea. [8]Petroleum and Marine Research Division, Korea Institute of Geoscience and Mineral Resources, 34132, Daejeon, South Korea. *email: sinam@kopri.re.kr

| Characteristics | Wijdefjorden | Dicksonfjorden | Hornsund |
|---|---|---|---|
| Latitude (°N) | 79.0~80.3 | 78.4~78.8 | 69.3~77.1 |
| Longitude (°E) | 15.4~16.2 | 15.3~15.4 | 15.8~16.7 |
| Range of water depth (m) | 112~322 | 37~109 | 37~193 |
| Bedrock Lithology[66] | Phyllite sandstone | Sandstone, black mudstone & calcareous shale | Phyllite, Mesozoic shales & sandstones |
| Age[66] | Meso/Paleozoic & Devonian | Carboniferous/ Permian & Devonian | Neoproterozoic & Jurassic/ Cretaceous |
| Glacier fed-system | Marine terminating | Land terminating | Marine terminating |
| Summer temperature (°C) | −3~−1 | 0~1 | 2~3 |
| Catchment area (km$^2$) | 1,100[21] | 1,013[67] | >1,200[30] |
| Total glacier area (km$^2$) | 500 | 283 | 802* |
| Loss balance of glacier mass[¥] (w. eq. m yr$^{-1}$) | −0.26 | −0.26 | −0.55 |
| Annual loss glacier volume (km$^3$ yr$^{-1}$) | 0.13 | 0.07 | 0.44 |
| Glacier retreat rate (m yr$^{-1}$) | <10 | 35 | 70 |
| Glacier retreat area rate (km$^2$ yr$^{-1}$) | — | 0.24 | 1.6 |
| Sedimentation rate (cm yr$^{-1}$) | 0.01[20,68] | 0.1~0.4[69] | 0.17~0.66[22] |
| Mass accumulation rate in sediment[§] (g m$^{-2}$ yr$^{-1}$) | 40 | 1100 | 1800 |
| OC accumulation rate in sediment[£] (g m$^{-2}$ yr$^{-1}$) | 0.3~0.8 | 1.3~11.3 | 9.3~49.4 |

**Table 1.** Physical, geological[52] and glacier[21,30,31,62–65] properties and surface organic carbon (OC) accumulation rates of the Wijdefjorden, Dicksonfjorden and Hornsund surface sediments in the Svalbard archipelago. *Area of tidewater glacier is 781 km$^2$. [¥]These values were estimated using a geodetic method comparing the glacier thickness over years in the maps of a glacier made at two different points in time. [§]Mass accumulation rate (MAR) was calculated using the following equation: MAR (g cm$^{-2}$ yr$^{-1}$) = Sedimentation rate (cm yr$^{-1}$) × [1-Porosity] × Bulk density (g cm$^{-3}$) We used 0.7 and 1.85 (g cm$^{-3}$) for porosity[18] and bulk density[18,20], respectively. [£]OC accumulation rate was calculated by multiplying OC by MAR.

environments[18,19]. Given that Hg demonstrates a strong binding affinity towards organic matter (OM), we investigated the influence of OM on the spatial distribution of THg in the fjord systems. To address this research, we collected 35 surface sediment samples from three fjords in Spitsbergen that are affected by various glacial influences: Wijdefjorden in the northern Spitsbergen, Dicksonfjorden in the central Spitsbergen and Hornsund in the southern Spitsbergen. Each study area is characterized by distinct glacier dynamics, bedrock lithology, and oceanic currents with meltwaters. The THg, total organic carbon (TOC), total nitrogen (TN), and total sulfur (TS) contents, and their isotope values were analyzed in the surface sediments. Six trace metals (As, Cu, Ni, Zn, Cr, and Pb) and twelve proxy tracers, which indicate the influence of weathering and redox processes, were also analyzed to examine the potential controlling factors for the spatial distribution of THg in fjord surface sediments. Our study examines the sources and factors that influence the deposition (i.e., sediment composition, runoff, weathering, and anthropogenic influence), and the spatial distribution of Hg in fjord sediments in the Svalbard archipelago.

## Results

### Geological and glacier properties, and organic carbon (OC) accumulation rates.
The bedrock mainly represents Paleozoic strata in Wijdefjorden and Dicksonfjorden, and Mesozoic strata in Hornsund (Table 1). Therefore, the bedrock components in Hornsund are relatively younger compared to other fjords. The glacier-fed systems were marine-terminating types for Wijdefjorden and Hornsund, whereas Dicksonfjorden had a land-terminating glacier-fed system. The total glacier area, the annual loss glacier volume, and the glacier retreat rate were significantly higher in Hornsund than Wijdefjorden and Dicksonfjorden (Table 1). Furthermore, sedimentation and OC accumulation rates were higher in Hornsund compared to other fjords (Table 1)[20–24]. However, sedimentation rates can exceed several tens of cm yr$^{-1}$ in the vicinity of terrestrial sources[25,26].

### THg and other trace metal concentrations.
The THg concentrations in the surface sediments were the highest in Hornsund (52 ± 15 ng g$^{-1}$, $n = 21$), followed by Wijdefjorden (30 ± 9 ng g$^{-1}$, $n = 6$), and Dicksonfjorden (16 ± 6 ng g$^{-1}$, $n = 8$) (Table 2). The average THg concentration in Hornsund surface sediment was three times higher than in Dicksonfjorden. The highest THg concentrations occurred in Brepollen, a bay surrounded by retreating tidewater glaciers in the innermost parts of Hornsund (Fig. 1 and Table S1). The THg mass accumulation rate in Hornsund (92 ± 27 μg m$^{-2}$ yr$^{-1}$) was higher than those of Wijdefjorden (1.2 ± 0.4 μg m$^{-2}$ yr$^{-1}$) and Dicksonfjorden (17 ± 6 μg m$^{-2}$ yr$^{-1}$) in Svalbard. The THg mass accumulation rate in Hornsund was comparable to that of the Huang He River (100 ± 15 μg m$^{-2}$ yr$^{-1}$), which is well known for high sedimentary Hg accumulation rates due to industrial and riverine input, but much higher compared to East China (36 ± 2 μg m$^{-2}$ yr$^{-1}$) and Yellow seas (29 ± 2 μg m$^{-2}$ yr$^{-1}$) (Table 3).

The THg concentration in Wijdefjorden showed a decreasing trend from terrestrial to coastal (offshore) regions. The THg concentrations in Dicksonfjorden were relatively constant throughout the study area (Fig. 1). Other trace metal concentrations, including As, Cu, Ni, Zn and Cr were higher in Hornsund than in Wijdefjorden and Dicksonfjorden; however, Pb concentrations were not significantly different among the sites (Fig. 2).

| | THg in sediments (ng g$^{-1}$) | THg in rock[52] (ng g$^{-1}$) | TOC (%) | TN (%) | TS (%) | TOC/TN ratio | δ$^{13}$Corg (‰) | δ$^{15}$N (‰) | δ$^{34}$S (‰) |
|---|---|---|---|---|---|---|---|---|---|
| Wijdefjorden | 30 ± 9 | 0~0.89 | 1.20 ± 0.54 | 0.14 ± 0.10 | 0.15 ± 0.06 | 8.5 ± 0.5 | −23~−22 | 4.7~5.3 | 8~15 |
| Dicksonfjorden | 16 ± 6 | 5~13 | 0.59 ± 0.33 | 0.07 ± 0.03 | 0.09 ± 0.04 | 7.8 ± 2.4 | −25~−24 | 2.7~5.4 | 14~17 |
| Hornsund | 52 ± 15 | 0~0.89 | 1.68 ± 0.55 | 0.11 ± 0.03 | 0.25 ± 0.10 | 14.5 ± 2.8 | −27~−24 | 2.0~5.9 | −10~15 |

**Table 2.** Averages or range of chemical properties of surface sediments from Wijdefjorden, Dicksonfjorden, and Hornsund in the Svalbard archipelago.
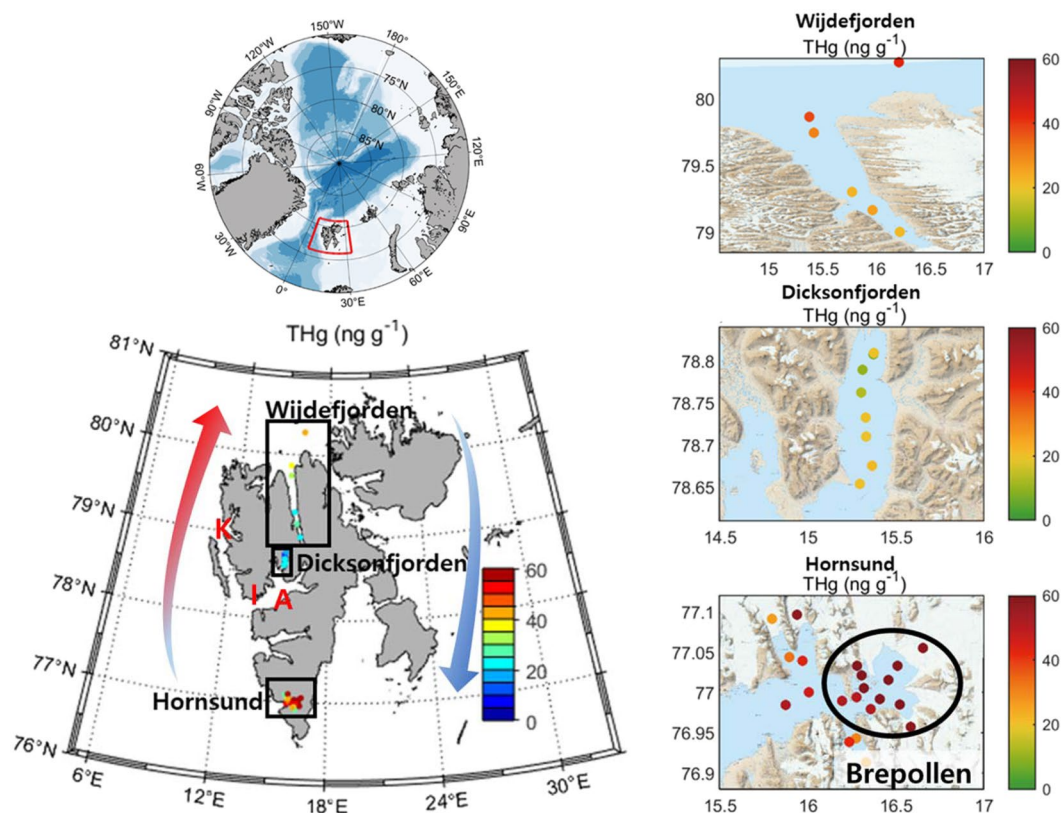


**Figure 1.** Spatial distributions of absolute THg concentration in the surface sediment of the Wijdefjorden, Dicksonfjorden, and Hornsund of Svalbard archipelago. The K, I, and A mean Kongsfjorden, Isfjorden, and Adventfjord, respectively. Red and blue arrows indicate warm Atlantic and cold Arctic currents, respectively. The map was created using an S100 Raster Data Set[70] in Matlab 2018a version[71].

**Correlation between THg, TOC and TS concentrations.** The concentrations of TOC (1.68 ± 0.55%, $n = 21$) and TS (0.25 ± 0.10%, $n = 20$) and TOC/TN ratios (14.5 ± 2.8, $n = 21$) were the highest in Hornsund, followed by Wijdefjorden (TOC; 1.2 ± 0.54%, $n = 6$, TS; 0.15 ± 0.06, $n = 3$, TOC/TN ratio 8.5 ± 0.5, $n = 6$), and Dicksonfjorden (TOC; 0.59 ± 0.33%, $n = 8$, TS; 0.09 ± 0.04%, $n = 6$, TOC/TN ratio 7.4 ± 2.4, $n = 8$) (Table 2 and S1). The average δ$^{13}$C$_{org}$ value was the highest in Wijdefjorden (ranging from −23 to −22‰, average of −22.8 ± 0.4‰, $n = 6$), followed by Dicksonfjorden (ranging from −25 to −24‰, average of −24.5 ± 0.5‰, $n = 8$), and Hornsund (ranging from −27 to −24‰, average of −25.6 ± 0.7‰, $n = 21$) (Table 2 and S1). The average δ$^{34}$S value was notably lower in Hornsund (ranging from −10 to 15‰, average of 1.3 ± 8.2‰, $n = 20$) compared to other sites (Wijdefjorden: ranging from 8 to 15‰, average of 10.9 ± 3.8‰, $n = 3$; and Dicksonfjorden, ranging from 14 to 17‰, average of 15.6 ± 1.2, $n = 6$) (Tables 2 and S1).

In all fjord systems studied, the concentrations of TOC (Fig. 3A) and TS (Fig. 3B) were strongly correlated with THg concentrations. The positive relationships between TOC and THg remained valid after THg and TOC values of individual sediments ([THg]$_{sample}$ and [TOC]$_{sample}$) were normalized to mean fjord values ([THg]$_{Fjord mean}$ and [TOC]$_{Fjord mean}$) (Fig. S1). The TOC/TN ratios also correlated well with THg concentration (Fig. 4B). Interestingly, the THg in Hornsund had a positive relationship with the TOC/TN ratio, ranging from 10 to 20. Wijdefjorden and Dicksonfjorden also showed positive correlations between THg concentrations and TOC/TN ratios with ratios less than 10 (Fig. 4B).

**Relative percentage of terrestrially-derived TOC.** The Hornsund sediments had relatively negative δ$^{13}$C (‰) values similar to the endmembers for terrestrially-derived OM, while the Wijdefjorden and

| Sites* | Sample No. | THg (ng g⁻¹) | MAR (g cm⁻² yr⁻¹) | THg MAR (μg m⁻² yr⁻¹) |
|---|---|---|---|---|
| Huang He River | 22 | $20 \pm 3$ | 0.5 | $100 \pm 15$ |
| Changjiang River | 24 | $105 \pm 11$ | 0.87 | $914 \pm 96$ |
| East China Sea | 27 | $18 \pm 1$ | 0.2 | $36 \pm 2$ |
| Yellow Sea | 195 | $19 \pm 1$ | 0.15 | $29 \pm 2$ |
| East Sea | 6 | $89 \pm 22$ | 0.02 | $18 \pm 4$ |
| Okhotsk Sea | 27 | $91 \pm 30$ | 0.02 | $18 \pm 6$ |
| Bering Sea | 11 | $49 \pm 9$ | 0.07 | $34 \pm 6$ |
| Western Arctic Ocean | 7 | $78 \pm 8$ | 0.04 | $31 \pm 3$ |
| Alaska permafrost[37] | 588 | $43 \pm 30$ | — | — |
| Wijdefjorden | 6 | $30 \pm 9$ | 0.004 | $1.2 \pm 0.4$ |
| Dicksonfjorden | 8 | $18 \pm 7$ | 0.11 | $17 \pm 6$ |
| Hornsund | 21 | $52 \pm 15$ | 0.18 | $92 \pm 27$ |

**Table 3.** THg concentrations and THg mass accumulation rates in surface sediments from various sites. *The data from Huang He River, Changjiang River, East China Sea, East Sea, Okhotsk Sea, Bering Sea and western Arctic Ocean were referred from Kim *et al.*[38].

Dicksonfjorden had higher $\delta^{13}C$ (‰) values, characterized by marine-derived OM (Fig. 4A–C). Using the $\delta^{13}C$ (‰) endmembers for terrestrial and marine sources (see Eqs. 1 and 2 in the Methods section), the Hornsund sediment was composed of a relatively high proportion of terrestrial OM ($F_{terr}$; an average of $78 \pm 17\%$ terrestrial source) (Fig. 4C). The relative contribution of terrestrial OM to surface sediments ($F_{terr}$) decreased with increasing latitude, suggesting that TOC in the Wijdefjorden sediments was predominantly composed of marine OM (with an average of 35% terrestrial sources and 65% marine sources) (Fig. 4C). In addition, 14 out of 20 sites in the Hornsund studied showed depleted $\delta^{34}S$ (‰) values, which were within the endmember of terrestrially derived-OM (Fig. 4D).

**Relationships between detrital/redox proxy metals and THg concentrations.** To investigate the effects of weathering (or erosion) on THg concentrations, THg was plotted with detrital and lithogenic proxy metals such as Al, Zr, Ti, Rb, Th and Hf, which are often used as indicators of these influences[27–29]. Our results showed positive relationships between the concentrations of THg, Zr, Ti and Hf across all sites ($p < 0.05$; Table 4 and S2). To investigate the effect of anaerobic reduction on THg concentrations, redox proxy metals including Fe, Mn, Cr, V, Mo and U, were plotted with THg concentrations. The results indicated positive correlations between THg, Cr and V concentrations in the surface sediments of the Svalbard fjords (Tables S3, $p < 0.05$). The discussion of redox influence on spatial THg distributions was described in the supplementary information in detail.

## Discussion

Hornsund has one of the largest areas of glacier coverage in the catchment area and a broad calving front in the Svalbard fjord systems[30,31]. Since the 1990s, the Hornsund glaciers have retreated rapidly in Svalbard (~70 m yr⁻¹ on average) and had a large annual volume of loss glaciers (0.44 km³ yr⁻¹ on average) due to higher summer temperature (by 2~3 °C) compared to other fjords[30,31]. Therefore, Hornsund with tidewater glaciers is particularly susceptible to the influence of glacier melting, which releases fresh meltwater and drifting ice to fjords. These processes have shown to supply modern and ancient OM, trace metals, and nutrients both directly by releasing glacier-trap resources and indirectly by exposing terrestrial landscape prone to runoff to fjord ecosystems[32,33]. In fact, high sediment (0.17 ~ 0.66 cm yr⁻¹) and organic carbon (OC) accumulation (9.3 ~ 49.4 g m⁻² yr⁻¹) rates were observed in Hornsund. The THg concentrations ($52 \pm 15$ ng g⁻¹) and THg mass accumulation rates (THg MAR) in Hornsund ($94 \pm 27$ μg m⁻² yr⁻¹) were comparable to those of Huang He River (THg; $20 \pm 15$ ng g⁻¹, THg MAR; $100 \pm 15$ μg m⁻² yr⁻¹) and higher than East China (THg; $18 \pm 1$ ng g⁻¹, THg MAR; $36 \pm 29$ μg m⁻² yr⁻¹) and Yellow Seas (THg; $19 \pm 1$ ng g⁻¹, THg MAR; $29 \pm 2$ μg m⁻² yr⁻¹), which are characterized by substantial coastal runoff and the largest local anthropogenic Hg emission in the world (Table 3). We speculate that the deglaciation is the main process leading to increased Hg release into the Svalbard fjord environment as supported by the elevated trace metal concentrations (As, Cu, Ni, Zn and Cr) and TOC in addition to THg in the Hornsund sediments.

The deglaciation-mediated Hg release to the Svalbard fjord environment is likely facilitated by OM. It has long been suggested that OM mediates the transport of Hg from terrestrial to the adjacent aquatic environment. Negatively charged surfaces of OM are enriched with carboxyl functional groups ($RCOO^-$), and thiolates ($RS^-$) in OM behave as ligands to form a transition metal thiolate complex, which leads to a strong binding affinity with trace metals including Hg[34–36]. These associations among OM, thiolates, and THg contents can explain the positive relationships among them as observed in the Svalbard fjords (Fig. 3). These results support earlier studies showing that sediments with high OM are typically characterized by high Hg concentrations in the North Slope of Alaska, the Yukon River basin in the Canadian Arctic, and Kongsfjorden on Spitsbergen[10,16,37,38].

The observed TOC/TN ratios and the $\delta^{13}C$ values of the sediments suggest that Hg bound to terrestrial OM, which is either released directly via glacial meltwater or indirectly by exposing terrestrial landscape, acts as the primary Hg source to the Hornsund sediments in contrast to other locations of Wijdefjorden and Dicksonfjorden.
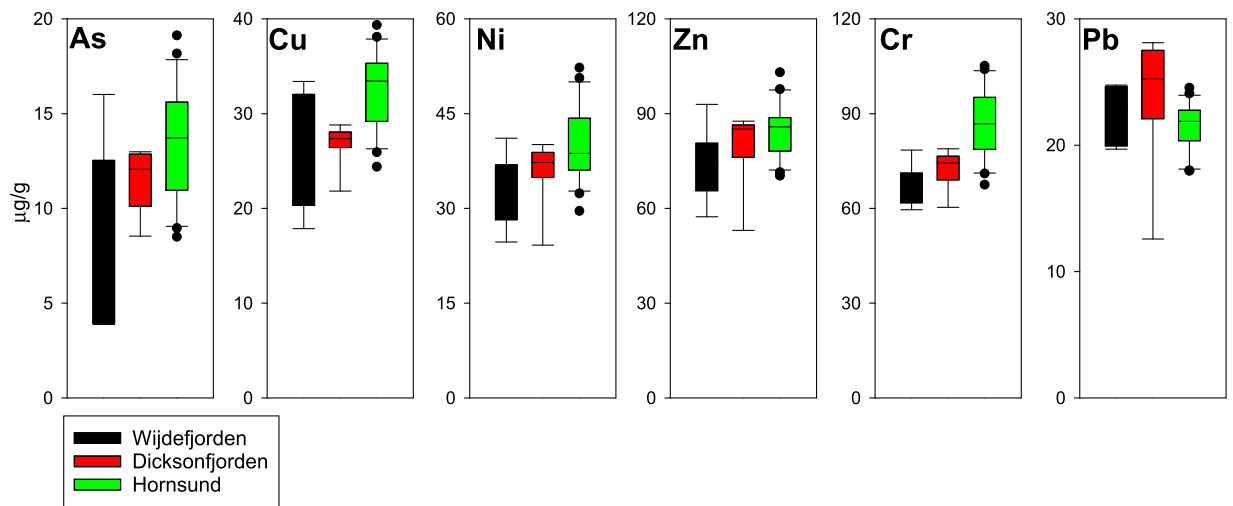
**Figure 2.** Box plots of trace metal concentrations (As, Cu, Ni, Zn, Cr, and Pb) in the surface sediments of the Svalbard fjords that were studied.
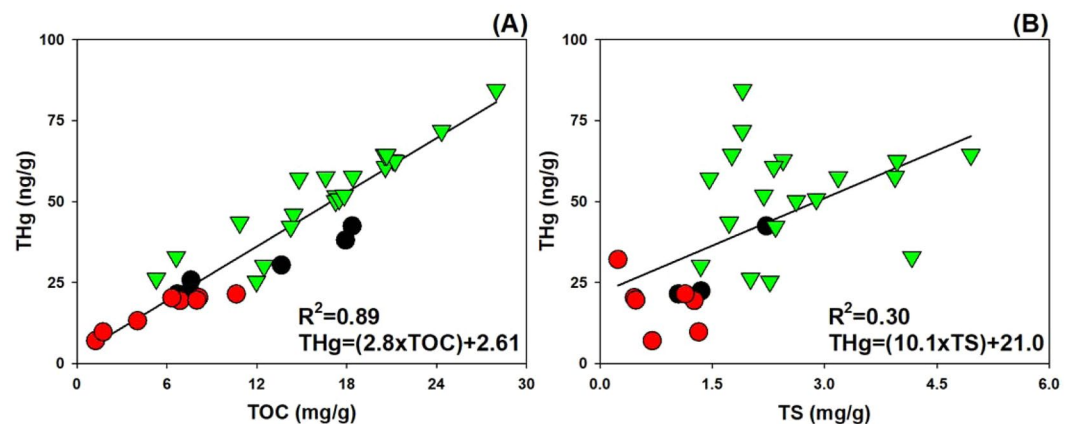


**Figure 3.** Relationships between TOC (**A**), TS (**B**) and THg concentrations of the surface sediments in the Svalbard fjords that were studied.

Terrestrially-derived OM has a TOC/TN ratio larger than 10 and a $\delta^{13}C$ value ranging from $-29.3$ to $-25.5‰$ in the Arctic, due to the influence of $C_3$ plants and ancient OM[39–43]. The OM from marine sources displays a lower TOC/TN ratio (i.e., <8) and a heavier $\delta^{13}C$ value ($> -25‰$)[42–46]. Our results suggest that OM in the Hornsund sediments, which display relatively high TOC/TN ratios and relatively depleted $\delta^{13}C$ values, is mainly derived from modern and ancient terrestrial OM (Fig. 4A,B). The Hornsund sediments also had the highest THg concentration. The Wijdefjorden sediments consist mainly of OM originated from marine sources (Fig. 4A,B). The Dicksonfjorden sediments, which have average values for both TOC/TN ratio and $\delta^{13}C$, were probably generated by the mixing of both terrestrially- and marine-derived OM (Fig. 4A,B).

To quantify the contribution of terrestrially-derived OM to fjord sediments, we calculated $F_{terr}$ (the percentage of terrestrial OM in the samples) using the $\delta^{13}C$ (‰) end members derived from terrestrial and marine sources[39]. Due to the complex lithology of the Svalbard fjord sediments, which can lead to an extensive range of $\delta^{13}C$ end members for terrestrial OM, we used measured $\delta^{13}C$ end members from Spitsbergen (Hornsund and Adventfjord) for terrestrial sources, and sites west of Svalbard for marine sources (45 samples collected in the open ocean off Svalbard), and calculated a mixing model with C and N isotopes, and TOC/TN ratios[43,47,48]. The results indicated that the Hornsund sediments were composed of both modern and ancient terrestrial OM (78%), which is consistent with earlier studies[22,43,48]. The contribution of OM derived from marine sources was relatively higher in the Wijdefjorden (65%) and Dicksonfjorden (37%) sediments (Fig. 4C). This finding implies that the sediments in Hornsund are influenced by OM carried in meltwater from glaciers, which promotes the release of Hg bound to OM from terrestrial sources.

To support our hypotheses that OM in Hornsund mostly came from terrestrial sources, we further analyzed the isotopic values of sulfur ($\delta^{34}S$) (Fig. 4D). The $\delta^{34}S$ values have been used as a tool for distinguishing terrestrial OM from marine-derived OM. The $\delta^{34}S$ values of terrestrially- and marine-derived OM have larger differences compared to $\delta^{13}C$ values, and the assimilation and degradation of OM lead to a smaller degree of $\delta^{34}S$ fractionation

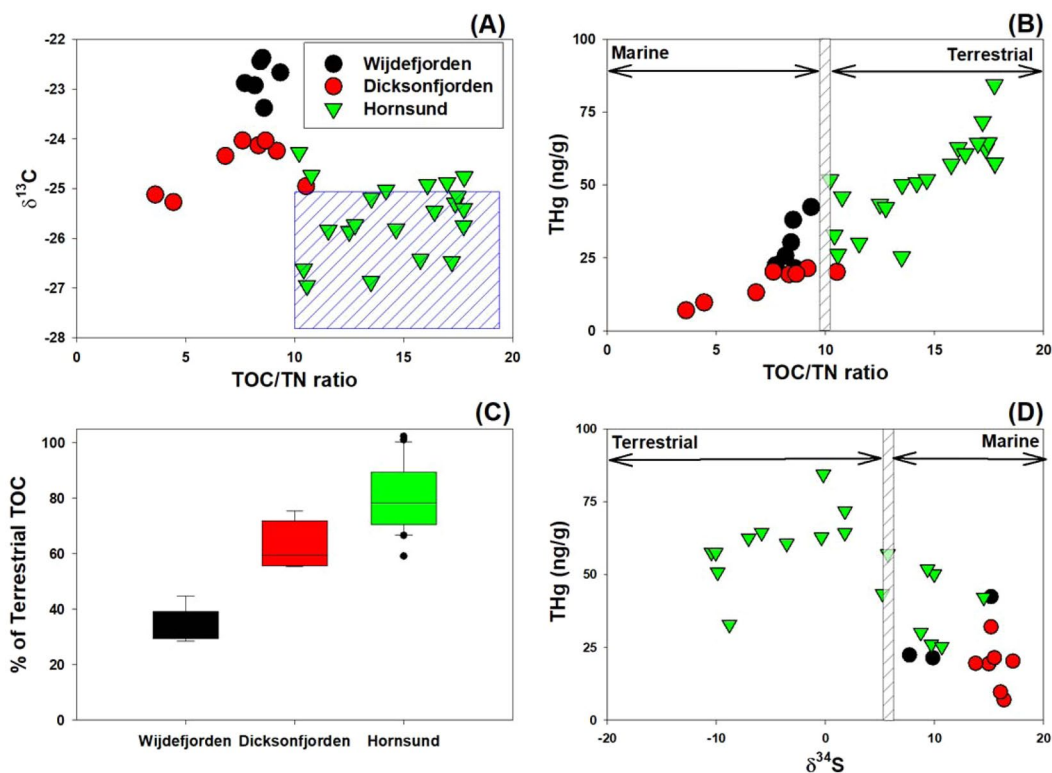**Figure 4.** Relationship between TOC/TN ratio and δ¹³C values (‰) (**A**), THg and TOC/TN ratios (**B**), the percentage of terrestrial organic carbon ($F_{terr}$; **C**), and THg and δ³⁴S (‰) values (**D**) in the surface sediments in the Svalbard fjords studied. The blue box (**A**) indicates the range of TOC/TN ratio and δ¹³C (‰) that are derived from terrestrial OM.

| Other trace metals | | As | Cu | Ni | Zn | Cr | Pb |
|---|---|---|---|---|---|---|---|
| THg | R² | 0.54 | 0.45 | 0.08 | 0.13 | 0.53 | −0.04 |
| | P value | **<0.01** | **0.01** | 0.65 | 0.47 | **<0.01** | **0.02** |
| TOC | R² | 0.41 | 0.38 | 0.01 | 0.04 | 0.45 | −0.34 |
| | P value | **0.01** | **0.02** | 0.96 | 0.82 | **0.01** | 0.05 |
| **Detrital & Lithogenic weathering proxies** | | Al | Zr | Ti | Rb | Th | Hf |
| THg | R² | 0.28 | 0.41 | 0.41 | −0.22 | −0.29 | 0.56 |
| | P value | 0.11 | **0.01** | **0.01** | 0.21 | 0.09 | **<0.01** |
| TOC | R² | 0.26 | 0.52 | 0.46 | −0.21 | −0.26 | 0.61 |
| | P value | 0.13 | **<0.01** | **0.01** | 0.22 | 0.13 | **<0.01** |

**Table 4.** Pearson correlation coefficients and *p* values between THg, TOC, and metals in surface sediment from Svalbard fjords.

(by 1 ~ 2‰)[49,50]. Thus, δ³⁴S values can be a conservative tracer accounting for terrestrially- and marine-derived OM[51]. Generally, the terrestrially-derived OM has lower δ³⁴S values (6.3‰) compared to marine-derived OM (18.1‰)[49,50]. In our results, Hornsund had notably lower δ³⁴S isotopic values (ranging from −10 to 15‰, average of 1.3 ± 8.2‰, n = 20) than those of Wijdefjorden (ranging from 8 to 15‰, average of 10.9 ± 3.8‰, n = 3) and Dicksonfjorden (ranging from 14 to 17‰, average of 15.6 ± 1.2‰, n = 6), indicating that the surface sediment of Hornsund was mainly composed of terrestrial sources (Table 2 and Fig. 4D). In particular, lower δ³⁴S values in the Hornsund were mainly observed in the inner part of fjord, Brepollen, which had high THg concentration and was significantly affected by tidewater glaciers (Fig. 1).

While terrestrially-derived OM is thought to be the main mediator for the transport of Hg to the Svalbard fjord sediments, the source of Hg still remains a question. Fjord sediments have been shown to receive Hg via three major sources-direct atmospheric deposition (in the form of precipitation), industrial runoff, and riverine input. The fjord sediments in Svalbard are atypical such that there are few major point sources of anthropogenic Hg. The recent records of atmospheric Hg deposition in the Arctic region (>5 ug m⁻² yr⁻¹) have also

shown particularly low values compared to other regions of the world (East China and Yellow seas: 86 ~ 133 ug $m^{-2}$ $yr^{-1}$) but the THg concentration of the Svalbard fjord sediments are comparable to several remote regions (Table 3)[8,9,38]. Based on a number of analyses performed in this study, we speculate that the dominant Hg source to the Svalbard sediments is through weathering of bedrock. Although the THg concentrations in the bedrock were higher in Dicksonfjorden than Wijdefjorden and Hornsund (Table 2), Ottesen *et al.*[52] reported that the Jurassic or Cretaceous and Triassic bedrock in Hornsund contain higher Hg concentrations (ranging from 40 to 80 ng g$^{-1}$) compared to the Devonian rock in the Wijdefjorden and Dicksonfjorden (ranging from 5 to 30 ng g$^{-1}$)[52]. To assess the contribution of weathering or erosion, we analyzed the detrital metals degraded from bedrocks (Al, Zr, Ti, Rb, Th and Hf), which are the most abundant components of minerals, less immobile in sediments and exclusively derived from natural sources (i.e., no anthropogenic source exists)[29,53]. Observed positive relationships between THg and some detrital proxies (Zr, Ti, Hf) suggest that weathering or erosion may have liberated Hg, which is then sequestered and transported by terrestrially-derived OM to the sediment (Table 3). Bełdowski *et al.*[15] also report a noticeable impact of weathered bedrock minerals on sediment THg concentration that were transferred from glacial meltwater in Kongsfjorden as well as in Hornsund. It should also be noted that the rapid deglaciation event has likely facilitated the erosion of bedrock particularly in Hornsund, which explains the highest THg observed in that location. In summary, the lithogenic characteristic such as bedrock composition and degree of weathering or erosion could be one of the significant factors determining the spatial THg distribution in the sediment.

Given the absence of local or regional anthropogenic disturbances (which are described in the supplementary information in detail), another natural Hg source to the Svalbard fjord sediments is by sinking of particulate OM. A recent study[54] has suggested that high Hg concentrations observed in lake sediments located near Ny-Ålesund are caused by increased phytoplankton biomass due to global warming. Phytoplankton carcasses can take up Hg from the water column and subsequently deposited Hg directly into the sediment[54]. Based on the relatively heavier $\delta^{13}$C values and lower TOC/TN ratios[39,43], which are indicators of the influence of marine phytoplankton, it is possible that algal scavenging processes have influenced the Wijdefjorden and Dicksonfjorden sediments in recent periods. This process, however, does not explain the elevated sediment THg concentration in Hornsund, which is mainly consisted of terrestrial OM

In summary, Hornsund experiencing rapid glacial retreat rates and a wide calving front showed the highest concentrations of THg ($52 \pm 15$ ng g$^{-1}$) and TOC ($1.68 \pm 0.55\%$), compared to the Wijdefjorden and Dicksonfjorden fjords. Our study suggests that the sedimentary THg contents of all three fjords are mainly derived from weathered and deposited minerals, and both modern and ancient OM released from melting glaciers act as the primary transport mechanism for Hg. Thus, the large amount of THg released from the terrestrial to the fjord system is likely to affect Hg cycling in the water column as well as the sediments of the Svalbard fjords.

## Methods

### Site description and sampling.
Spitsbergen is the largest island of the Svalbard archipelago, located approximately 76° to 81°N and 10° to 28°E (Fig. 1). The exact location and detailed information on geological settings of the study areas are listed in Tables 1 and S1. Spitsbergen is surrounded by the European Arctic Ocean, the Greenland Sea and the Barents Sea, and it is affected by three major oceanic currents; i.e., the West Spitsbergen Current (WSC), which transports relatively warm and saline Atlantic Water, and the East Spitsbergen (ESC) and Sørkapp currents (SC), which carry colder and fresher Arctic Water (Fig. 1)[55]. The fjords contain locally produced surface, intermediate and winter-cooled waters, which are influenced by the melting of glaciers and sea-ice, local precipitation and riverine runoff[11]. Whereas Wijdefjorden and Dicksonfjorden receive the WSC, Hornsund is influenced by both the warm current of the WSC and the cold current of the ESC. Furthermore, Wijdefjorden and Hornsund receive relatively large volumes of runoff from tidewater glaciers and glacifluvial rivers, whereas Dicksonfjorden only receives runoff from glacifluvial rivers[56,57].

Surface sediment samples were collected from 35 stations located in Wijdefjorden ($n = 6$; water depths 112–322 m), Dicksonfjorden ($n = 8$; water depth 37–109 m) and Hornsund ($n = 21$; water depth 37–193 m) during three marine geological cruises on R/V Helmer Hanssen in September 2015, July 2016 and July 2017. The samples were collected using a box corer (W50 cm × H50 cm × D50 cm) (Table S1). Sub-samples were taken from the upper 1 cm of all box cores from Wijdefjorden and Dicksonfjorden, as well as from three cores from Hornsund. However, 18 sub-samples collected from the Hornsund cores during the cruise in 2015 were taken from a sediment depth range of 0–5 cm. There was no significant difference in chemical properties (THg, total organic carbon, total organic nitrogen, and $\delta^{13}$C values) between the 1 cm and 0–5 cm depth samples from Hornsund, indicating that samples of 0–5 cm depth have similar properties to the surface sediments. All subsamples were freeze-dried for two days and then ground to a powder using a mortar and pestle before further analyses.

Four bedrock samples of phyllite sandstone, calcareous shale, and black mudstone were obtained from an archive of Svalbard bedrocks that were collected during field campaigns led by the Korea Polar Research Institute from 2013 to 2015, in the Isfjorden area and central Spitsbergen. The analyzed rocks have similar compositions to the rocks surrounding our study sites (Table 1). The rock samples were also ground to powder using a ball mill.

### Analyses of THg, major and trace elements.
Total Hg (THg) concentrations for surface sediments and bedrock samples were measured at the Library for Marine Samples (LIMS), KIOST and the Gwangju Institute of Science and Technology, using an automatic Hg analyzer, which undergoes thermal decomposition followed by catalytic reduction, amalgamation, desorption, and an atomic absorption module (model Hydra II Direct Hg analyzer; Teledyne Leeman Labs, Hudson, NH, USA). The THg concentrations were calibrated against marine sediment reference materials (MESS-3) for trace metals and other constituents (National Research Council of Canada). The analytical accuracies were determined to be <5%, based on replicate analyses of certified reference

materials, and the analytical precision of the THg concentration measurement was determined to be <10%, based on replicate measurements of standard materials and sediment samples. To determine the concentrations of Al, Zr, Ti, Rb, Hf, Fe, Mn, Cr, V, Mo and U, the powdered samples were dissolved with a standard reference material (MAG-1) in a mixture of hydrofluoric and perchloric acids, and the elemental concentrations were measured using inductively coupled plasma atomic emission spectroscopy (Spectro Flame Modula EOP; SPECTRO Analytical Instruments Inc., Kleve, Germany) at the Korea Basic Science Institute. The analytical accuracy and precision ranged from 5 to 10%, and the concentrations were calibrated against Marine Sediment-1 reference material (certified by the U.S. Geological Survey)[58].

### Analyses of TOC, TN, TS, $\delta^{13}$C, $\delta^{15}$N, and $\delta^{34}$S.

The concentrations of total carbon (TC), total nitrogen (TN), total sulfur (TS) and total inorganic carbon (TIC) in the dried and ground sediment samples were measured using a Thermo Electron Corporation Flash EA 1112 Series NC Soil Analyzer for TC and TN, an organic elemental analyzer for TS (Vario Micro cube, Elementar, Germany), and a $CO_2$ coulometer (model CM5014; UIC Inc.) for TIC (Waltham, MA, USA), at the Library for Marine Samples (LIMS), KIOST. The accuracy and precision in the analysis of these elements were <5%, based on analysis of standard reference materials ($_L$-cysteine in the TC and TN analyses, sulfanilamide and acetanilide in the TS analysis, and calcium carbonate having 12% C in the TIC analysis). TOC concentrations were calculated by subtracting TIC from TC[59].

For the carbon stable isotope analyses of OM, all sediment samples were treated with a 1 M HCl solution to remove $CaCO_3$, while the $\delta^{15}$N samples were not acid-treated. The $\delta^{13}$C and $\delta^{15}$N values were measured using a CN elemental analyzer (Thermo Electron Corporation Flash EA 2000, Thermo Fisher Scientific, Germany) coupled with an isotope ratio mass spectrometer (Finnigan Delta Plus, Thermo Fisher Scientific, Germany) at the Korea Polar Research Institute[60]. The measurement error was <0.2‰ for carbon and <0.3‰ for nitrogen, and the $\delta^{13}$C and $\delta^{15}$N values were reported relative to the $\delta^{13}$C value for PDB (Pee Dee Belemnite) and air, respectively. The PDB standard and air were calibrated relative to Indiana University Acetanilide #1, USGS40, USGS41, Urea, and Thermo Soil Stand.

The sulfur (TS) contents and its isotopic value ($\delta^{34}$S) were measured with bulk sediment samples using a CNS elemental analyzer (Vario Micro cube, Elementar, Germany) coupled with a stable isotope ratio mass spectrometer (Isoprime100, Elementar, Germany) at the Korea Institute of Geoscience and Mineral Resources (KIGAM). Replicated analyses had a precision of better than 0.6%. The Vienna-Canyon Diablo Troilite (VCDT) was used for standardizing the material, and it was calibrated with NBS127 as reference.

### Calculation of the percentage for terrestrial organic carbon.

Terrestrial OM is isotopically lighter (ranging from −29.3 to −25.5‰, median value = −27.3‰) than marine OM (ranging from −17 to −25‰, median value = −21‰), because $C_3$ plants predominate on land over $C_4$ plants at high latitudes[40,41,43,47]. In a simplified case, the use of these two endmembers allows the calculations of fractions of terrestrial or marine OM, respectively. However, the fjords on Svalbard receive not only modern terrestrial OM but also ancient OM derived from sedimentary rocks with variable $\delta^{13}$C values, depending on their origin[24]. Moreover, in regions such as the inner part of Hornsund fjord, almost the entire catchment area is covered by glaciers, cutting off any source of modern terrestrial OM[24]. The $\delta^{13}$C values for terrestrial runoff can also be affected by excrement from bird colonies, which were frequently observed in the vicinity of the Svalbard fjords. It has been reported that $\delta^{13}$C is about −26.6‰[61]. Therefore, the calculated terrestrial OM fraction must be considered as a simplified approximation.

For the calculations, we used a $\delta^{13}$C of −26.8‰ for the terrestrial OM endmember[43,47,48], and −20.6‰ for the marine OM in the Spitsbergen fjords[43,47,48]. Using these C isotope endmember values, we calculated the relative contribution of terrestrial OM ($F_{terr}$) to fjord sediments using the following equations:[45]

$$\sigma 13C_{org(sample)} = F_{terr} \times \sigma 13C_{org(terrestrial)} + (1 - F_{terr}) \times \sigma 13C_{org(marine)} \tag{1}$$

$$F_{terr}(\%) = \frac{\sigma 13C_{org(sample)} - \sigma 13C_{org(marine)}}{\sigma 13C_{org(terrestrial)} - \sigma 13C_{org(marine)}} \times 100(\%) \tag{2}$$

Where; $F_{terr}$ (%) is the percentage of terrestrial organic carbon in the samples, $\delta^{13}$C$_{org(sample)}$ is $\delta^{13}$C measured in the samples, and $\delta^{13}$C$_{org(terrestrial)}$ and $\delta^{13}$C$_{org(marine)}$ are the endmember values for terrestrial and marine OM as provided above.

### Statistical methods.

The distribution of THg in Fig. 1 was created from an S100 Raster Data Set (Norwegian Polar Institute 1990) and plotted in Matlab (Version 2018). The other plots were made using a sigma plot and R software (Version 13.0; Figs. 2–4, and S1). The statistical comparison between chemical parameters and THg contents were performed using the R software.

### References

1. Fitzgerald, W. F. *et al.* Modern and Historic Atmospheric Mercury Fluxes in Northern Alaska: Global Sources and Arctic Depletion. *Environ. Sci. Technol.* **39**, 557–568, https://doi.org/10.1021/es049128x (2005).
2. Gamberg, M., Chételat, J., Poulain, A. J., Zdanowicz, C. & Zheng, J. Mercury in the Canadian Arctic Terrestrial Environment: An Update. *Sci. Total Environ.* **509–510**, 28–40, https://doi.org/10.1016/j.scitotenv.2014.04.070 (2015).
3. Dastoor, A. *et al.* Atmospheric mercury in the Canadian Arctic. Part II: Insight from modeling. *Sci. Total Environ.* **509–510**, 16–27, https://doi.org/10.1016/j.scitotenv.2014.10.112 (2015).

4. Halbach, K., Mikkelsen, Ø., Berg, T. & Steinnes, E. The presence of mercury and other trace metals in surface soils in the Norwegian Arctic. *Chemosphere* **188**, 567–574, https://doi.org/10.1016/j.chemosphere.2017.09.012 (2017).

5. Steffen, A. *et al*. A synthesis of atmospheric mercury depletion event chemistry in the atmosphere and snow. *Atmos. Chem. Phys.* **8**, 1445–1482, https://doi.org/10.5194/acp-8-1445-2008 (2008).

6. Belicka, L. L. & Harvey, H. R. The sequestration of terrestrial organic carbon in Arctic Ocean sediments: A comparison of methods and implications for regional carbon budgets. *Geochimi. Cosmochim. Acta* **73**, 6231–6248, https://doi.org/10.1016/j.gca.2009.07.020 (2009).

7. Carignan, J. & Sonke, J. The effect of atmospheric mercury depletion events on the net deposition flux around Hudson Bay, Canada. *Atmos. Environ.* **44**, 4372–4379, https://doi.org/10.1016/j.atmosenv.2010.07.052 (2010).

8. Zhang, Y. *et al*. Observed decrease in atmospheric mercury explained by global decline in anthropogenic emissions. *P. Natl. Acad. Sci. USA* **113**, 526–531, https://doi.org/10.1073/pnas.1516312113 (2016).

9. Amos, H. M. *et al*. Global Biogeochemical Implications of Mercury Discharges from Rivers and Sediment Burial. *Environ. Sci. Technol.* **48**, 9514–9522, https://doi.org/10.1021/es502134t (2014).

10. Schuster, P. F. *et al*. Mercury export from the Yukon River Basin and potential response to a changing climate. *Environ. Sci. Technol.* **45**, 9262–9267, https://doi.org/10.1021/es202068b (2011).

11. Svendsen, H. *et al*. The physical environment of Kongsfjorden–Krossfjorden, an Arctic fjord system in Svalbard. *Polar Res.* **21**, 133–166, https://doi.org/10.1111/j.1751-8369.2002.tb00072.x (2002).

12. Siegel, F. R., Galasso, J. L., Kravitz, J. H. & Basinger, W. D. The Svalbard western coast: site of baseline geochemistry and incipient contamination. *Environ. Geol.* **39**, 816–822, https://doi.org/10.1007/s002540050498 (2000).

13. Birks, H., Jones, V. J. & Rose, N. Recent Environmental Change and Atmospheric Contamination on Svalbard as Recorded in Lake Sediments–Synthesis and General Conclusions. *J. Paleolimnol.* **31**, 531–546, https://doi.org/10.1023/B:JOPL.0000022550.81129.1a (2004).

14. Drevnick, P. E., Yang, H., Lamborg, C. H. & Rose, N. L. Net atmospheric mercury deposition to Svalbard: Estimates from lacustrine sediments. *Atmos. Environ.* **59**, 509–513, https://doi.org/10.1016/j.atmosenv.2012.05.048 (2012).

15. Bełdowski, J., Miotk, M., Zaborska, A. & Pempkowiak, J. Distribution of sedimentary mercury off Svalbard, European Arctic. *Chemosphere* **122**, 190–198, https://doi.org/10.1016/j.chemosphere.2014.11.050 (2015).

16. Liu, Y. *et al*. Total mercury and methylmercury distributions in surface sediments from Kongsfjorden, Svalbard, Norwegian. *Arctic. Environ. Sci. Pollut. Int.* **22**, 8603–8610, https://doi.org/10.1007/s11356-014-3942-0 (2015).

17. Mohan, M. *et al*. Rate of sediment accumulation and historic metal contamination in a tidewater glacier fjord, Svalbard. *Mar. Pollut. Bull.* **131**, 453–459, https://doi.org/10.1016/j.marpolbul.2018.04.057 (2018).

18. Smith, R. W., Bianchi, T. S., Allison, M., Savage, C. & Galy, V. High rates of organic carbon burial in fjord sediments globally. *Nat. Geosci.* **8**, 450, https://doi.org/10.1038/ngeo2421 (2015).

19. Cui, X., Bianchi, T. S., Savage, C. & Smith, R. W. Organic carbon burial in fjords: Terrestrial versus marine inputs. *Earth Planet. Sci. Lett.* **451**, 41–50, https://doi.org/10.1016/j.epsl.2016.07.003 (2016).

20. Elverhøi, A., Lønne, Ø. & Seland, R. Glaciomarine sedimentation in a modern fjord environment, Spitsbergen. *Polar Res.* **1**, 127–150, https://doi.org/10.1111/j.1751-8369.1983.tb00697.x (1983).

21. Joo, Y. J. *et al*. Holocene envrionmental changes in Dicksonfjorden, west Spitsbergen, Svalbard. *Polar Res.* **38**, 3426, https://doi.org/10.33265/polar.v383.3426 (2019).

22. Zaborska, A., Beszczyńska-Möller, A. & Włodarska-Kowalczuk, M. History of heavy metal accumulation in the Svalbard area: Distribution, origin and transport pathways. *Environ. Pollut.* **231**, 437–450, https://doi.org/10.1016/j.envpol.2017.08.042 (2017).

23. Zaborska, A. *et al*. Sedimentary organic matter sources, benthic consumption and burial in west Spitsbergen fjords–Signs of maturing of Arctic fjordic systems? *J. Marine Syst.* **180**, 112–123, https://doi.org/10.1016/j.jmarsys.2016.11.005 (2018).

24. Szczuciński, W. *et al*. Warming-controlled glaciers retreat and enhanced carbon burial-is there a negative feedback effect?-summary of multidisciplinary study in fjords of Svlabrd. *European Geoscience Union General Assembly* (Vienna, Austria, 2018).

25. Filipowicz, C. Textural parameters and classification of deposits in the modern glaciomarine environment, Hornsund Fjord, Spitsbergen. *Acta Geol. Pol.* **40**, 29–67 (1990).

26. Ćwiąkała, J. *et al*. Submarine geomorphology at the front of the retreating Hansbreen tidewater glacier, Hornsund fjord, southwest Spitsbergen. *J. Maps* **14**, 123–134, https://doi.org/10.1080/17445647.2018.1441757 (2018).

27. Hermanns, Y. M. & Biester, H. Anthropogenic mercury signals in lake sediments from southernmost Patagonia, Chile. *Sci. Total Environ.* **445–446**, 126–135, https://doi.org/10.1016/j.scitotenv.2012.12.034 (2013).

28. Loring, D. H. & Rantala, R. T. T. Manual for the geochemical analyses of marine sediments and suspended particulate matter. *Earth-Sci. Rev.* **32**, 235–283, https://doi.org/10.1016/0012-8252(92)90001-A (1992).

29. Cole, D. B., Zhang, S. & Planavsky, N. J. A new estimate of detrital redox-sensitive metal concentrations and variability in fluxes to marine sediments. *Geochim. Cosmochim. Acta* **215**, 337–353, https://doi.org/10.1016/j.gca.2017.08.004 (2017).

30. Małgorzata, B., Jacek, A. J. & Leszek, K. Fluctuations of tidewater glaciers in Hornsund Fjord (Southern Svalbard) since the beginning of the 20th century. *Polar Res.* **34**, 327–352, https://doi.org/10.2478/popore-2013-0024 (2013).

31. Nuth, C. *et al*. Decadal changes from a multi-temporal glacier inventory of Svalbard. *The Cryosphere* **7**, 1603–1621, https://doi.org/10.5194/tc-7-1603-2013 (2013).

32. Meire, L. *et al*. Spring bloom dynamics in a subarctic fjord influenced by tidewater outlet glaciers (Godthåbsfjord, SW Greenland). *J. Geophys. Res.: Biogeo.* **121**, 1581–1592, https://doi.org/10.1002/2015JG003240 (2016).

33. Moskalik, M. *et al*. Spatiotemporal changes in the concentration and composition of suspended particulate matter in front of Hansbreen, a tidewater glacier in Svalbard. *Oceanologia* **60**, 446–463, https://doi.org/10.1016/j.oceano.2018.03.001 (2018).

34. Skyllberg, U., Bloom, P. R., Qian, J., Lin, C.-M. & Bleam, W. F. Complexation of Mercury(II) in Soil Organic Matter: EXAFS Evidence for Linear Two-Coordination with Reduced Sulfur Groups. *Environ. Sci. Technol.* **40**, 4174–4180, https://doi.org/10.1021/es0600577 (2006).

35. Jiskra, M., Wiederhold, J. G., Skyllberg, U., Kronberg, R.-M. & Kretzschmar, R. Source tracing of natural organic matter bound mercury in boreal forest runoff with mercury stable isotopes. *Environmen. Sci.: Proc. Imp.* **19**, 1235–1248, https://doi.org/10.1039/C7EM00245A (2017).

36. Song, Y. *et al*. Thermodynamics of Hg(II) Bonding to Thiol Groups in Suwannee River Natural Organic Matter Resolved by Competitive Ligand Exchange, Hg LIII-Edge EXAFS and 1H NMR Spectroscopy. *Environ. Sci. Technol.* **52**, 8292–8301, https://doi.org/10.1021/acs.est.8b00919 (2018).

37. Schuster, P. F. *et al*. Permafrost Stores a Globally Significant Amount of Mercury. *Geophys. Res. Lett.* **45**, 1463–1471, https://doi.org/10.1002/2017GL075571 (2018).

38. Kim, H. *et al*. Increase in anthropogenic mercury in marginal sea sediments of the Northwest Pacific Ocean. *Sci. Total Environ.* **654**, 801–810, https://doi.org/10.1016/j.scitotenv.2018.11.076 (2019).

39. Meyers, P. A. Preservation of elemental and isotopic source identification of sedimentary organic matter. *Chem. Geol.* **114**, 289–302, https://doi.org/10.1016/0009-2541(94)90059-0 (1994).

40. Ruttenberg, K. C. & Goñi, M. A. Phosphorus distribution, C:N:P ratios, and $\delta^{13}C_{oc}$ in arctic, temperate, and tropical coastal sediments: tools for characterizing bulk sedimentary organic matter. *Mar. Geol.* **139**, 123–145, https://doi.org/10.1016/S0025-3227(96)00107-7 (1997).

41. Naidu, A. S. *et al*. Organic carbon isotope rations ($\delta^{13}C$) of Arctic Amerasian continental shelf sediments. *Int. J. Earth Sci.* **89**, 522–532, https://doi.org/10.1007/s005310000121 (2000).

42. Stein, A. & MacDonald, R. W. Organic carbon cycle in *the Arctic* Ocean (eds. Stein, A. & MacDonald, R. W.) (Springer, 2004).

43. Winkelmann, D. & Knies, J. Recent distribution and accumulation of organic carbon on the continental margin west off Spitsbergen. *Geochem. Geophy. Geosy.* **6**, Q09012, https://doi.org/10.1029/2005GC000916 (2005).

44. Sackett, W. Stable carbon isotope studies on organic matter in *The marine environments* (ed. Sackett, W.) (Elsevier Science, 1989).

45. Schubert, C. J. & Calvert, S. E. Nitrogen and carbon isotopic composition of marine and terrestrial organic matter in Arctic Ocean sediments:: implications for nutrient utilization and organic matter composition. *Deep Sea Res. Pt. I.* **48**, 789–810, https://doi.org/10.1016/S0967-0637(00)00069-8 (2001).

46. Khan, N. S., Vane, C. H., & Horton, B. P. Stable carbon isotope and C/N geochemistry of costal wetland sediments as a sea-level indicator in *Handbook of Sea-Level research* (eds. Shennan, I., Long, A. J. & Horton, B.) 295–311 (John Wiley and Sons, 2015).

47. Knies, J., Martinez, P. & Martinez, J. Organic matter sedimentation in the western Barents Sea region: Terrestrial and marine contribution based on isotopic composition and organic nitrogen content. *Norw. J. Geol.* **89**, 79–89 (2009).

48. Koziorowska, K., Kuliński, K. & Pempkowiak, J. Sedimentary organic matter in two Spitsbergen fjords: Terrestrial and marine contributions based on carbon and nitrogen contents and stable isotopes composition. *Cont. Shelf Res.* **113**, 38–46, https://doi.org/10.1016/j.csr.2015.11.010 (2016).

49. Peterson, B. J., Howarth, R. W. & Garritt, R. H. Multiple Stable Isotopes Used to Trace the Flow of Organic Matter in Estuarine Food Webs. *Science* **227**, 1361–1363 (1985).

50. Peterson, B. J. & Fry, B. Stable Isotopes in Ecosystems Studies. *Annu. Rev. Ecol. Syst.* **18**, 293–320, https://doi.org/10.1146/annurev.es.18.110187.001453 (1987).

51. Alling, V., Humborg, C., Mörth, C.-M., Rahm, L. & Pollehne, F. Tracing terrestrial organic matter by $\delta^{34}S$ and $\delta^{13}C$ signatures in a subarctic estuary. *Limnol. Oceanogr.* **53**, 2594–2602, https://doi.org/10.4319/lo.2008.53.6.2594 (2008).

52. Ottesen, R. T. *et al.* Part 2: Geochemical atlas of Spitsbergen in *Chemical composition of overbank sediments* (ed. Ottesen, R. T.) (Geological Survey of Norway Trondheim Norges geologiske undersokelse, 2010).

53. Boës, X., Rydberg, J., Martinez-Cortizas, A., Bindler, R. & Renberg, I. Evaluation of conservative lithogenic elements (Ti, Zr, Al, and Rb) to study anthropogenic element enrichments in lake sediments. *J. Paleolimnol.* **46**, 75, https://doi.org/10.1007/s10933-011-9515-z (2011).

54. Jiang, S., Liu, X. & Chen, Q. Distribution of total mercury and methylmercury in lake sediments in Arctic Ny-Ålesund. *Chemosphere* **83**, 1108–1116, https://doi.org/10.1016/j.chemosphere.2011.01.031 (2011).

55. Walczowski, W. & Piechura, J. New evidence of warming propagating toward the Arctic Ocean. *Geophys. Res. Lett.* **33**, https://doi.org/10.1029/2006GL025872 (2006).

56. Cottier, F. *et al.* Water mass modification in an Arctic fjord through cross-shelf exchange: The seasonal hydrography of Kongsfjorden, Svalbard. *J. Geophys. Res.* **110**, https://doi.org/10.1029/2004JC002757 (2005).

57. Promińska, A., Falck, E. & Walczowski, W. Interannual variability in hydrography and water mass distribution in Hornsund, an Arctic fjord in Svalbard. *Polar Res.* **37**, 1495546, https://doi.org/10.1080/17518369.2018.1495546 (2018).

58. Lim, D.-I., Jung, H. S., Kim, K. T., Shin, H. H. & Jung, S. W. Sedimentary records of metal contamination and eutrophication in Jinhae-Masan Bay, Korea. *Mar. Pollut. Bull.* **64**, 2542–2548, https://doi.org/10.1016/j.marpolbul.2012.07.033 (2012).

59. Sparks, D.R. Part 3. Chemical methods in *Methods of soil analysis* (ed. Sparks, D.R.) (Madison, Soil Science Socity of America, 1996).

60. Sharp, Z. Principles of stable isotope geochemistry (ed. Sharp, Z) (Prentice Hall, 2005).

61. Kuliński, K., Kędra, M., Legeżyńska, J., Gluchowska, M. & Zaborska, A. Particulate organic matter sinks and sources in high Arctic fjord. *J. Marine Syst.* **139**, 27–37, https://doi.org/10.1016/j.jmarsys.2014.04.018 (2014).

62. Małecki, J. Elevation and volume changes of seven Dickson Land glaciers, Svalbard, 1960–1990–2009. *Polar Res.* **32**, 18400, https://doi.org/10.3402/polar.v32i0.18400 (2013).

63. Hagen, J. O., Kohler, J., Melvold, K. & Winther, J. G. Glaciers in Svalbard: mass balance, runoff and freshwater flux. *Polar Res.* **22**, 145–159, https://doi.org/10.3402/polar.v22i2.6452 (2003).

64. Rachlewicz, G. River floods in glacier-covered catchments of the High Arctic: Billefjorden–Wijdefjorden, Svalbard. *Nork. Geogr. Tidsskr.* **63**, 115–122, https://doi.org/10.1080/00291950902907835 (2009).

65. D'Angelo, A. *et al.* Multi-year particle fluxes in Kongsfjorden, Svalbard. *Biogeosciences* **15**, 5343–5363, https://doi.org/10.5194/bg-15-5343-2018 (2018).

66. Dallmann, W. K. Chapter 7 Bedrock geology in Geoscience Atlas of Svalbard in *Norwegian Polar Institute Report* Series 148. (ed. Dallmann, W. K.) (Norwegian Polar Institute, 2015).

67. Bukowska-Jania, E. & Szafraniec, J. Distribution and morphometric characteristics of icing fields in Svalbard. *Polar Res.* **24**, 41–53, https://doi.org/10.3402/polar.v24i1.6252 (2005).

68. Bartels, M. *et al.* Atlantic Water advection vs. glacier dynamics in northern Spitsbergen since early deglaciation. *Clim. Past* **13**, 1717–1749, https://doi.org/10.5194/cp-13-1717-2017 (2017).

69. Kvam, M.H. Deposits and processes on the tide-influenced fjord head delta in Diskconfjorden, Svlabard in *Master theis in Sedimentology and Quanternary Geology* (The Arctic University of Norway, (2018).

70. Norewegian Polar Insitutue. S100 Raster Data Set in Norwegian Polar Data sets. *figshare* https://data.npolar.no/dataset/44ca8c2a-22c2-49e8-a50b-972734f287e3 (1990).

71. MATLAB and Statistics Toolbox Release R2018a. (The MathWorks, Inc., Natick, Massachusetts, 2018).

### Acknowledgements

### Author contributions

H.K. and S.N. designed the study and wrote the manuscript. S.N., D.L., S.H., and J.L. performed the sampling collection and analyses of chemical properties. Conversely, S.K., K.L., D.L., S.H., Y.J., and M.K. contributed to the manuscript with discussions and comments, and the statistical analyses and plotting of graphs were performed by T.K.

### Competing interests

The authors declare no competing interests.

## Additional information

**Supplementary information** is available for this paper at https://doi.org/10.1038/s41598-020-60261-6.

**Correspondence** and requests for materials should be addressed to S.-I.N.

**Reprints and permissions information** is available at www.nature.com/reprints.

**Publisher's note** Springer Nature remains neutral with regard to jurisdictional claims in published maps and institutional affiliations.